Effect of a large-amplitude circularly polarized wave on linear beam-plasma electromagnetic instabilities

L. Gomberoff and J. Hoyos
Departamento Física, Facultad de Ciencias, Universidad de Chile, Santiago, Chile

A. L. Brinca
Centro de Física de Plasmas, Instituto Superior Técnico, Lisbon, Portugal

Received 16 July 2003; revised 24 September 2003; accepted 4 November 2003; published 31 December 2003.

[1] In a previous paper, sufficiently large-amplitude and left-handed "pump waves" propagating parallel to the background magnetic field were shown to stabilize a moderately dense beam in a proton plasma against the generation of waves drawing their energy from the differential streaming motion of the beam [*Gomberoff*, 2003]. We now examine the general case of both left-hand and right-hand pump waves and their effects on beam instability as a function of pump wave amplitude and frequency, beam speed, and plasma component temperatures. We find that the left-hand pump wave always gives beam stability above a threshold amplitude. Larger threshold trend with increasing beam speed and lower ones with increasing temperature. It is also shown that they can stabilize left-hand polarized instabilities in the case of large drift velocities. The right-hand pump similarly suppresses beam instabilities when its pump frequency is below the linearly unstable range of frequencies. However, when its pump frequency is within the range of instability, that part of the range below the pump frequency is stabilized beyond a threshold amplitude, but the part above becomes even more unstable in the presence of a right-hand pump. *INDEX TERMS:* 7839 Space Plasma Physics: Nonlinear phenomena; 7867 Space Plasma Physics: Wave/particle interactions; 7868 Space Plasma Physics: Wave/wave interactions; 7871 Space Plasma Physics: Waves and instabilities; 2164 Interplanetary Physics: Solar wind plasma; *KEYWORDS:* nonlinear waves, beam-plasma instabilities, left and right-handed linear waves, instability thresholds, Alfvén/ion cyclotron waves

Citation: Gomberoff, L., J. Hoyos, and A. L. Brinca, Effect of a large-amplitude circularly polarized wave on linear beam-plasma electromagnetic instabilities, *J. Geophys. Res.*, *108*(A12), 1472, doi:10.1029/2003JA010144, 2003.

1. Introduction

[2] Electromagnetic ion beam-plasma interactions take place in various space and astrophysics environments as well as in laboratory plasmas. Proton beams have been observed in several regions of space, and in some places they display very large drift velocities (e.g., upstream of the quasi-perpendicular bow shock where $U \leq 10$. U is the beam drift velocity normalized to the Alfvén velocity) [see, e.g., *Hoppe et al.*, 1981, 1982; *Leubner and Viñas*, 1986; *Marsch*, 1991; *Gary*, 1991].

[3] In the linear theory, these waves have been studied both numerically and analytically by many authors [see, e.g., *Gary*, 1991; *Gomberoff and Elgueta*, 1991; *Gnavi et al.*, 1996; *Gomberoff et al.*, 1996; *Gomberoff and Astudillo*, 1998; *Gomberoff et al.*, 2000]. The growth rates of the instability maximize parallel to the background magnetic field.

[4] The nonlinear behaviour of finite amplitude and circularly polarized waves which propagate parallel to the background magnetic field involve parametric wave-wave interactions and also effects on beam components when present. The latter effects are the subject of this paper. Nonlinear behavior of left-hand polarized electromagnetic waves in a solar wind-like plasma involving alpha particles drifting relative to the proton, have been studied by *Hollweg et al.* [1993] and *Gomberoff et al.* [1994]. Studies of parametric decays of right-hand waves have been carried out by *Hollweg* [1994] [see also *Jayanti and Hollweg*, 1994a, 1994b]. Their nonlinear evolution has also been studied by using drift kinetic effects [*Inhester*, 1990], and hybrid computer simulation techniques [*Vasquez*, 1995]. Studies including dissipation and varying beam drift speeds have been carried out by *Gomberoff* [2000] and *Gomberoff et al.* [2001, 2002]. The effect and evolution of the beam for right-hand and left-hand polarized waves have also been studied by using simulation experiments [see, e.g., *Daughton et al.*, 1999].

[5] In the work of *Gomberoff* [2003], it was shown that right-hand instabilities (r-instability) can be stabilized by large-amplitude Alfvén/ion-cyclotron waves. Here we investigate several situations involving left-handed and right-handed large-amplitude waves (L and R waves of large amplitude) in a system which is linearly unstable.

0148-0227/03/2003JA010144

Thus for example, in the work of *Gomberoff* [2003] the beam velocity was assumed constant. It is shown here that the threshold L-wave amplitude required to stabilize the linear r-instability increases with increasing beam velocity, and for fixed drift velocity, it decreases with increasing pump wave frequency. For beam drift speeds above the threshold required to destabilize l-instabilities, L-waves can also stabilize the l-instability. The mechanism is more efficient when the large-amplitude waves have frequencies closer to the proton gyrofrequncy.

[6] In the case when there is a large-amplitude R-wave in the system, it is shown that the part of the linear unstable spectrum below the wave frequency (which may involve r as well as l-instabilities depending on the beam drift velocity) can be completely stabilized for pump wave amplitudes above a threshold value. On the other hand, the spectrum above the pump wave frequency can be either destabilized further, or the whole corresponding dispersion branch can become unstable.

[7] The paper is organized as follows. In section 2, the linear beam-plasma dispersion relation in the cold approximation is briefly discussed, and a brief derivation of the nonlinear dispersion relation for L and R waves is presented. In section 3, the dispersion relation is solved graphically in a number of different situations in order to illustrate the various effects found. In section 4, the results are summarized and discussed.

2. Dispersion Relation

[8] The plasma dispersion relation for circularly polarized electromagnetic waves propagating in the direction of an external magnetic field in a system consisting of electrons, a proton core, and a proton beam, is given by [*Gomberoff*, 1992; *Gomberoff and Hernández*, 1992; *Gnavi et al.*, 1996; *Gomberoff and Astudillo*, 1996],

$$y_0^2 = \frac{x_0^2}{1-x_0} + \frac{\eta(x_0 - y_0 U)^2}{1-(x_0 - y_0 U)}. \tag{1}$$

where $x_0 = \omega_0/\Omega_p$, $y_0 = k_0 v_A/\Omega_p$, $v_A = B_0/(4\pi\, n_p M_p)^{1/2}$ is the Alfvén speed, $U = V/v_A$ is the normalized beam velocity, $\eta = n_b/n_c$ is the beam density relative to the core density, and $\Omega_p = qB_0/cM_p$ is the proton gyrofrequency.

[9] The dispersion relation, equation (1), is valid in a current-free plasma and in the reference frame where the proton core is at rest [*Gomberoff and Elgueta*, 1991]. For an alpha particle beam, the dispersion relation was first derived by using kinetic theory in the semicold approximation [*Gomberoff and Elgueta*, 1991] and later on by using fluid theory [*Hollweg et al.*, 1993]. The dispersion relation for an arbitrary ion beam can be found in the work of *Gomberoff* [1992].

[10] We now derive very briefly the nonlinear dispersion relation assuming the plasma to be composed by electrons, background protons, beam protons, and a left-hand circularly polarized wave propagating along the external magnetic field. This wave corresponds to the pump wave. Each plasma component satisfies the following fluid equation of motion,

$$\left(\frac{\partial}{\partial t} + u\cdot\nabla\right)\vec{u} = \frac{q_l}{m_l}\left(\vec{E} + \frac{1}{c}\vec{u}\times\vec{B}\right) - \frac{\vec{\nabla}p}{n_l m_l}, \tag{2}$$

where $\vec{u}$ is the bulk velocity, q_l is the electric charge, m_l is the mass, $\vec{E}$ and $\vec{B}$ are the electric and magnetic field, respectively, and p is the pressure.

[11] As pointed out before, the dispersion relation given by equation (1) was first derived by linearizing Vlasov's equation [*Gomberoff and Elgueta*, 1991], and using the semicold approximation. Later on, it was derived by using first-order perturbation theory on the fluid equation (2) for zero temperature [*Hollweg et al.*, 1993]. Finally, it was also shown to be an exact solution of equation (2) for zero pressure [*Gomberoff et al.*, 1994].

[12] Following a procedure similar to *Hollweg et al.* [1993] [see also *Gomberoff et al.*, 1994, 1995; *Gomberoff* 1995; *Galvão et al.*, 1996], the nonlinear dispersion relation can be written in the following form [*Gomberoff et al.*, 2002; *Gomberoff*, 2003],

$$L_+L_-D + L_+R_-B_{-cc} + L_+R_{-b}B_{-ccb} + L_-R_+B_+ + L_-R_{+b}B_{+b} + (B_{-cc}B_{+b} - B_{-ccb}B_+)(R_-R_{+b} - R_{-b}R_+)/D = 0. \tag{3}$$

In the last equation,

$$L_\pm = y_\pm^2 - x_\pm^2/\psi_\pm - \eta x_{\pm b}^2/\psi_{\pm b}$$

$$R_\pm = y_\pm\left(x_0 - \frac{yx_0^2}{y_0 x} + \frac{x_\pm}{\psi_\pm}\right)/2\psi_0$$

$$R_{\pm b} = \eta y_\pm\left(x_{0b} - \frac{yx_{0b}^2}{y_0 x_b} + \frac{x_{\pm b}}{\psi_{\pm b}}\right)/\psi_{0b}$$

$$D = \beta_e'\Delta\eta r_b x^2 + \beta_e'\Delta_b r x_b^2 - \Delta\Delta_b(x x_b)^2$$

$$B_+ = -\beta_e' B_{+b1}\eta r x x_b + B_{+1}x^2\left(\beta_e'\eta r_b - \Delta_b x_b^2\right)$$

$$B_{+b} = -\beta_e' B_{+1} r_b x x_b + B_{+b}x_b^2\left(\beta_e' r - \Delta x^2\right)$$

$$B_{-cc} = -\beta_e' B_{-ccb1}\eta r_b x x_b + B_{-cc1}x^2\left(\beta_e'\eta r_b - \Delta_b x_b^2\right)$$

$$B_{-ccb} = -\beta_e' B_{-cc1} r_b x x_b + B_{-ccb1}x_b^2\left(\beta_e' r - \Delta x^2\right)$$

$$B_{+(b)1} = -\frac{A\psi_{-(b)}\left(y_+\psi_{+(b)}x_{0(b)}^2 - y_0\psi_{0(b)}x_{+(b)}^2\right)}{y_0 y_+ x_{(b)}}$$

$$B_{-cc(b)1} = \frac{A\psi_{+(b)}\left(y_-\psi_{-(b)}x_{0(b)}^2 - y_0\psi_{0(b)}x_{-(b)}^2\right)}{y_0 y_- x_{(b)}}$$

$$\Delta = A + r\left(1 - \frac{\beta_p y^2}{x^2}\right)$$

$$\Delta_b = A + r_b\left(1 - \frac{\beta_b y^2}{x_b^2}\right)$$

$$\beta_l = 4\pi n_p \gamma K T_l/B_0^2 \;\; (l = e, c, b),$$

where $x = \omega/\Omega_p$, $y = kv_A/\Omega_p$, K is the Boltzmann constant, T_l is the temperature of species l, and

$$x_b = x - yU$$

$$x_{0b} = x_0 - y_0 U$$

$$A = (B/B_0)^2$$

$$r_{(b)} = \psi_{0(b)}\psi_{+(b)}\psi_{-(b)}$$

$$\psi_0 = 1 - x_0$$

$$\psi_{0b} = 1 - x_{0b}$$

$$\psi_{\pm} = 1 - x_{\pm}$$

$$\psi_{\pm b} = 1 - x_{\pm b}$$

$$x_{\pm} = x_0 \pm x$$

$$y_{\pm} = y_0 \pm y$$

$$x_{0b} = x_0 - y_0 U$$

$$x_{\pm b} = x_{\pm} - y_{\pm} U$$

$$\beta'_e = \beta_e y^2/(1+\eta).$$

[13] The pump wave is characterized by the coordinates x_0 and y_0, and it is at the origin of the (x, y) coordinate system. For zero pump intensity, $A = 0$, equation (3) reduces to $L_+L_-D = 0$. The solution $L_{\pm} = 0$, corresponds to the dispersion relation of the upper and lower side band waves, respectively. The other solution $D = 0$, corresponds to the sound waves present in the system which, for $\eta \ll 1$, are given by,

$$x \simeq \pm\left(\beta_e + \beta_p\right)^{1/2} y \tag{4}$$

$$(x - yU) \simeq \pm(\beta_b)^{1/2} y \tag{5}$$

[14] Equation (4) represents the ordinary ion-acoustic waves propagating forward and backward relative to the proton core, and equation (5) corresponds to ion-acoustic waves, supported mainly by the proton beam. They move forward and backward relative to the beam. The solutions of $L_{\pm} = 0$ give the various branches of the dispersion relation. The crossings between the solutions give the position and nature of the possible wave couplings of the system. The solutions of the nonlinear dispersion relation, equation (3), are invariant under a rotation through an angle of 180°. Therefore it is sufficient to analyze the solutions in the upper half $\omega - k$ plane [see, e.g., *Hollweg et al.*, 1993; *Jayanti and Hollweg*, 1994a, 1994b; *Gomberoff et al.*, 1994, 1995; *Gomberoff*, 2000; *Gomberoff et al.*, 2001]. Note that for $A = 0$, only the ion-acoustic modes depend on the temperature. Note also that the cold plasma dispersion relation for electromagnetic modes is a good approximation in those regions of space where $\beta_{\|i} = v_{th.i}/v_A \ll 1$ ($v_{th.i} = \sqrt{2KT(i)/M(i)}$ is the thermal velocity of species i). This may happen for small temperatures and also for not so small temperatures [see, e.g., *Gomberoff and Neira*, 1983; *Gomberoff*, 1992] or for very large Alfvén velocity relative to the thermal velocity, like, e.g., in coronal holes [see, e.g., *Cranmer*, 2002; *Hollweg and Isenberg*, 2002, and references therein]. Equation (3) corresponds to the dispersion relation for left-hand polarized nonlinear waves. The dispersion relation for R-waves of large amplitude can be obtained by replacing (x, y) by (−x, −y) and (x_0, y_0) by ($-x_0$, $-y_0$). Alternatively, one can simply take ($-x_0$, $-y_0$) for the frequency and wavenumber of the right-hand nonlinear wave and leave the rest unchanged. This is so because the (x, y) plane is invariant under rotations through an angle of 180°.

3. Numerical Study of the Nonlinear Dispersion Relation

[15] In order to study the nonlinear dispersion relation, equation (3), we use a graphical method first derived by *Longtin and Sonnerup* [1986].

3.1. L-Wave Effects on Beam Instability

[16] We start by studying the effect of varying beam velocity on the stabilization of the r-instability due to the presence of an L-wave. In the work of *Gomberoff* [2003] it was shown that for $\beta_i = 0.001$, $\eta = 0.2$, $U = 2$, a large-amplitude wave of frequency $x_0 = 0.1$ stabilizes the linear instability for $A_t = 0.16$, where A_t is the minimum amplitude of the pump wave required to stabilize the linear instability. As U increases, A_t is expected to increase too. In Figure 1a we illustrate the situation for $U = 2.3$ and $A = 0$. The gap between the two curves denoted by −F and −b corresponds to the r-instability and is shown by an arrow [see *Gomberoff*, 2003, Figure 1]. The lines denoted by −F and −b are lower right-hand polarized sideband waves propagating in the direction of the external magnetic field [see *Gomberoff*, 2003]. The labels of the various branches of the dispersion relation are given in Table 1. In Figure 1b, $A = 0.81$ and the gap between −F and −b has disappeared showing thereby complete stabilization of the linear instability. Thus the threshold amplitude is now $A_t = 0.81$, instead of $A_t = 0.16$ for $U = 2$, as expected [see *Gomberoff*, 2003]. It can be shown that in general, A_t increases with increasing U. On the other hand, if the pump wave frequency is increased, the threshold value decreases. In fact, in Figure 2a we have taken $x_0 = 0.5$, and $A = 0$. The arrow shows the linear instability gap. The other parameters are the same as in the previous figure. In Figure 2b, we have taken $A_t = 0.7$, and the instability is completely stabilized. Thus as the pump wave frequency increases, the threshold A_t-value decreases. In general, for fixed U, the instability threshold continues to decrease as the pump wave approaches the proton gyrofrequency. The effect is very pronounced for frequencies very close to the resonance. For example, for $U = 3$, and $x_0 = 0.3$, $A_t = 2.5$. However, for the same drift velocity but for $x_0 = 0.95$, $A_t = 0.47$. Finally, in Figure 3 we consider the case when $U = 2.8$. In this case there are are both r and l-instabilities. In Figure 3a we have plotted the nonlinear dispersion relation for $x_0 = 0.9$, and $A = 0$. The arrow shows the linear instability region. In Figure 3b, $A = 0.63$. The linear instability is completely stabilized, including the l-instability region corresponding to Alfvén waves. It is simple to show that the l-instability is the first to be stabilized as A increases.

3.2. R-Wave Effects on Beam Instability

[17] We shall now study the effect of a R-wave on the linear instability. To do this, as explained above, one can simply choose x_0 to be negative and leave the rest unchanged. Thus, we take a R-wave of frequency $x_0 = -0.1$. The other parameters are the same as in Figure 1. In Figure 4a we illustrate the linear instability for $A = 0$ and $U = 2$, and it is shown by the arrow. This corresponds to the gap involving

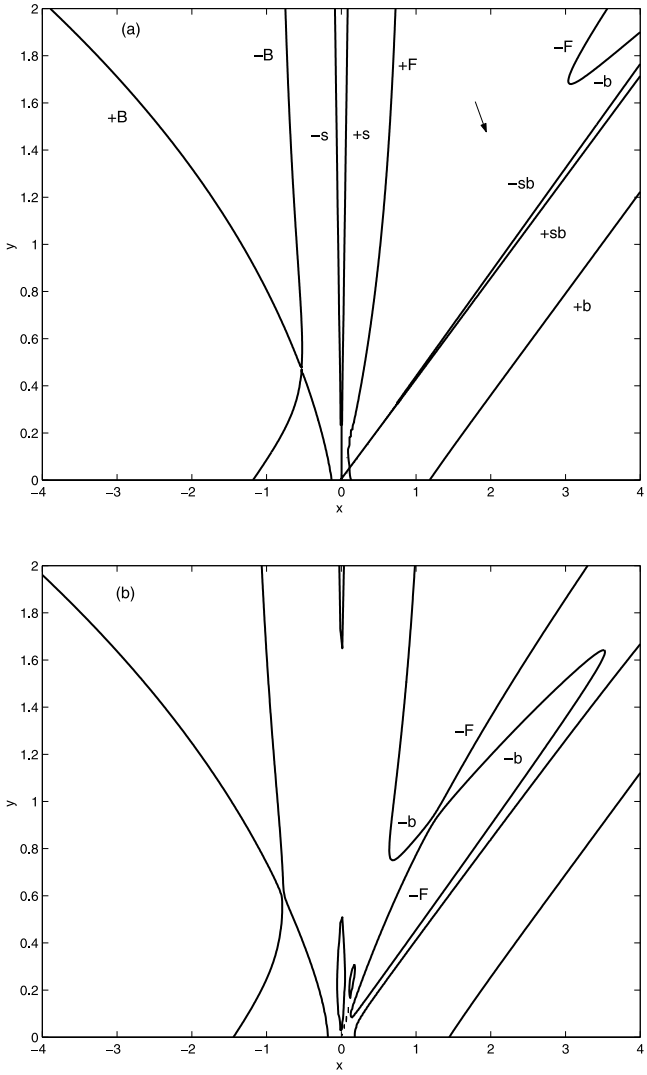

Figure 1. Nonlinear dispersion relation, equation (3), x versus y, for $\eta = 0.2$, $U = 2.3$, $\beta_i = 0.001$, $x_0 = 0.1$, for (a) $A = 0$, and (b) $A = 0.81$.

−F and −b. Note that these two roots correspond now to upper sideband waves while for a L-wave they correspond to lower sideband waves [*Gomberoff*, 2003]. In Figure 4b, A_t has been raised to $A = 0.146$. The gap has disappeared altogether indicating complete stabilization of the linear instability. This is a similar situation to *Gomberoff* [2003], but now the stabilization is due to the presence of a large amplitude R-wave. We shall now increase the beam drift velocity to $U = 4$. As shown in Figure 5a, there are several linear instability regions, right and left polarized. The regions between B and C and D and O are r-instabilities, while the region between O and G is a l-instability. In the following we study the effect of a R-wave on these instability regions. To this end, we take $x_0 = -0.1025$, with corresponding $y_0 = -0.1$. As it follows from Figure 5a, in this case the pump wave is unstable. In Figure 5b we show the nonlinear dispersion relation, equation (3), for $A = 0$. The other parameters are like in the previous figures. There are two right-hand polarized instability regions, one going from the origin to the point denoted by D and the other from the C to B. The other two instability regions cover the gap between the origin and the point denoted by G. In Figure 5c, we have raised the pump wave amplitude to $A = 0.1$, and we see that except for the region between the points D and C, the whole right-hand branch has been destabilized. In Figure 5d we have raised the pump wave amplitude further to $A = 0.21$, and one can see that even the small stable region between D and C is now unstable. In other words, for a R-wave with $A \geq 0.21$, the branch of the dispersion relation above the pump wave frequency is completely destabilized. In this case the

Table 1. Characterization of the Various Modes Appearing in Equation (3)[a]

Mode	Characterization
+ (−)F	lh (rh) forward propagating
+ (−) B	rh (lh) backward propagating
+ (−) b	lh (rh) forward propagating
+ (−) s	ion-acoustic forward (backward) propagation
+ (−) sb	beam ion-acoustic forward (backward) propagation

[a]The + (−) sign refers to the upper (lower) sideband waves and lh (rh)left-hand (right-hand) polarization. F refers to the branch of the pump wave, and b refers to the branch due to the beam.

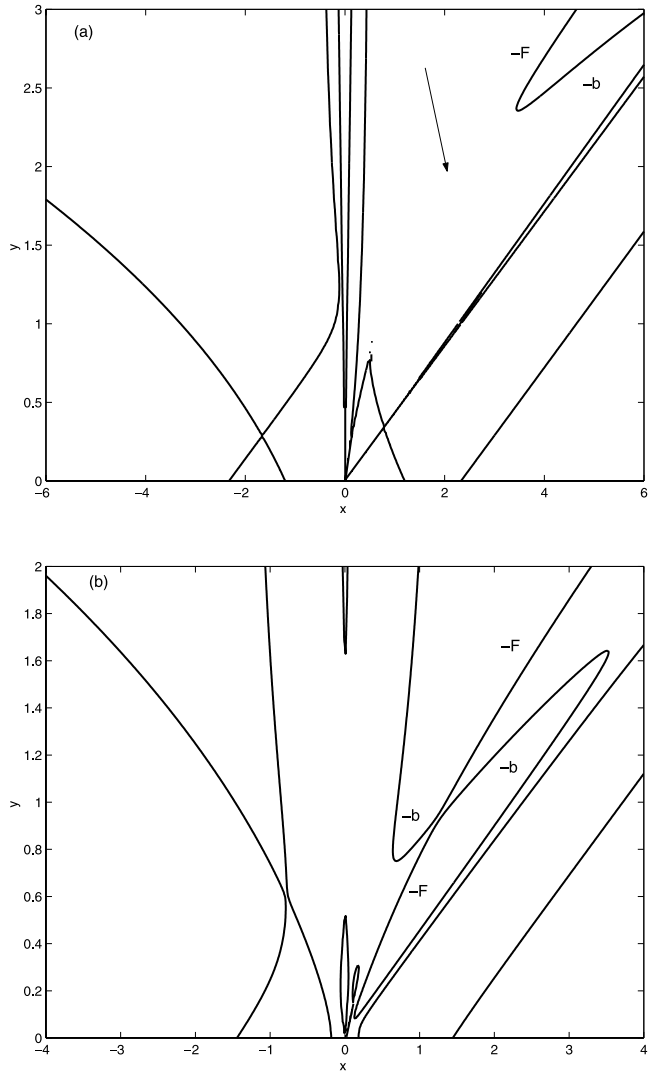

Figure 2. Same as Figure 1, but $x_0 = 0.5$ for (a) $A = 0$ and (b) $A = 0.7$.

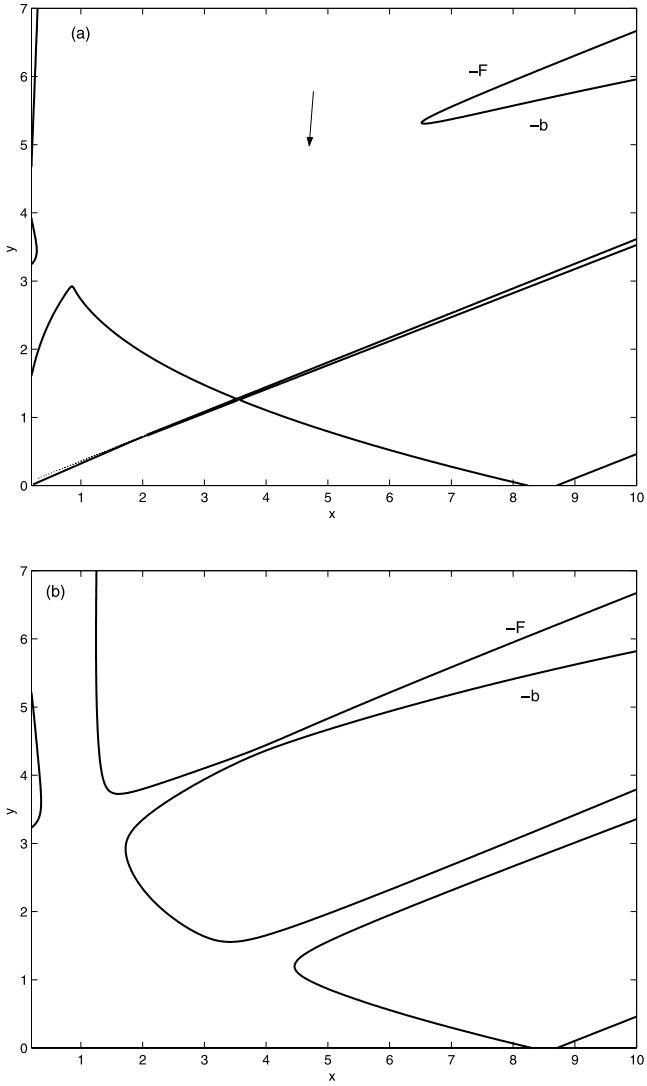

Figure 3. Nonlinear dispersion relation, equation (3), x vs. y, for $\eta = 0.2$, $U = 2.8$, $\beta_i = 0.001$, $x_0 = 0.9$, for (a) $A = 0$ and (b) $A = 0.63$.

pump wave acts in the opposite direction than the left hand pump, i.e., it helps the destabilization of the this branch. For the same parameters of Figure 5b, in Figure 6a we show again the dispersion relation x vs. y, and concentrate on the gap between the origin and the point denoted by G in Figure 5a. This region involves an right-instability which goes from the origin to the point $x = 0.1025$ and $y = 0.1$, and a l-instability going from this point to G. In Figure 6b, the pump wave amplitude has been raised to $A = 0.8$. From this figure it follows that the point G is now closer to the origin, showing stabilization of the l-instability. In Figure 6c, we have raised $A = 1.35$ in order to show that the whole region is now stable.

4. Discussion

[18] By solving graphically the nonlinear dispersion relation equation (3) [*Longtin and Sonnerup*, 1986], we have shown the following properties of a system containing a large amplitude circularly polarized wave propagating in a linearly unstable beam-plasma system. First, we assumed an L-wave and we showed that as the beam velocity increases the threshold A_t-value also increases. On the other hand, for fixed drift velocity, the threshold required to stabilize the linear r-instability decreases with increasing pump wave frequency. A third result found in this case is that even in the case when the drift velocity is large enough to trigger l-instabilities, these can also be stabilized by an L-wave. The stabilization process is more efficient for L-wave frequencies close to the proton gyrofrequency. In Table 2 the results are extended to various temperatures and pump wave frequencies for $U = 2.2$ and $U = 2.3$. As it follows from Table 3 of *Gomberoff* [2003] and the present Table 2, A_t increases with increasing drift velocity and decreases with increasing wave frequency for fixed drift velocity.

[19] Next, we studied the effect of finite amplitude R-waves on l and r-instabilities. This was done for two cases. First, we considered the case when the frequency of the pump wave is in a region where the system is linearly stable, and second in a region where the system is linearly unstable. In the first case, we showed that the presence of

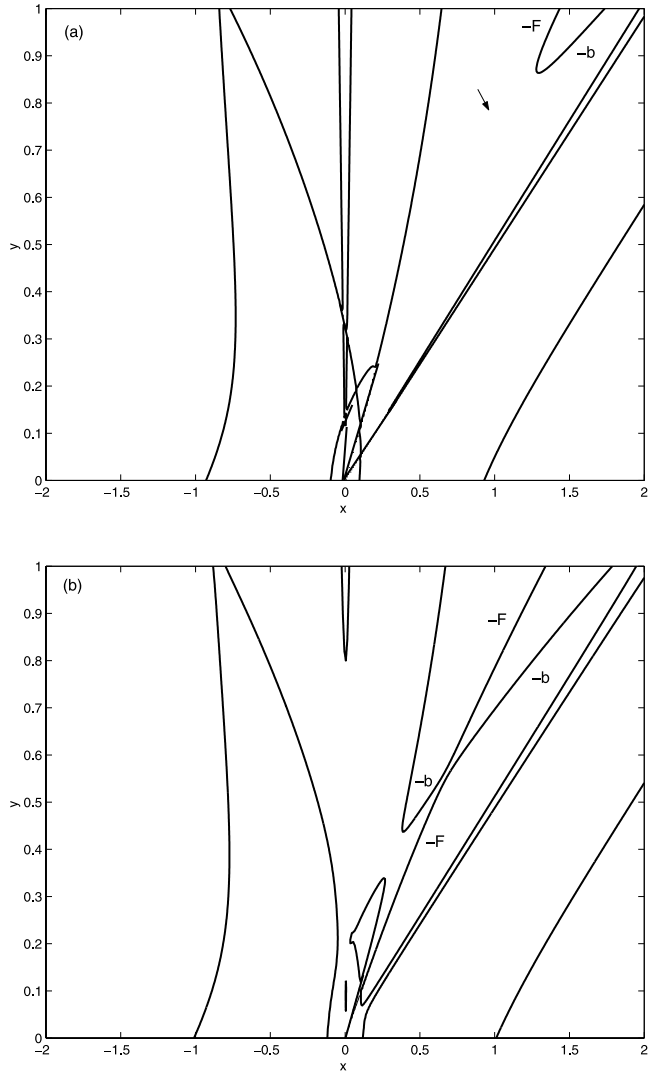

Figure 4. Same as Figure 1, but for a right-hand polarized pump of frequency $x_0 = 0.1$ and $U = 2$, for (a) $A = 0$ and (b) $A = 0146$.

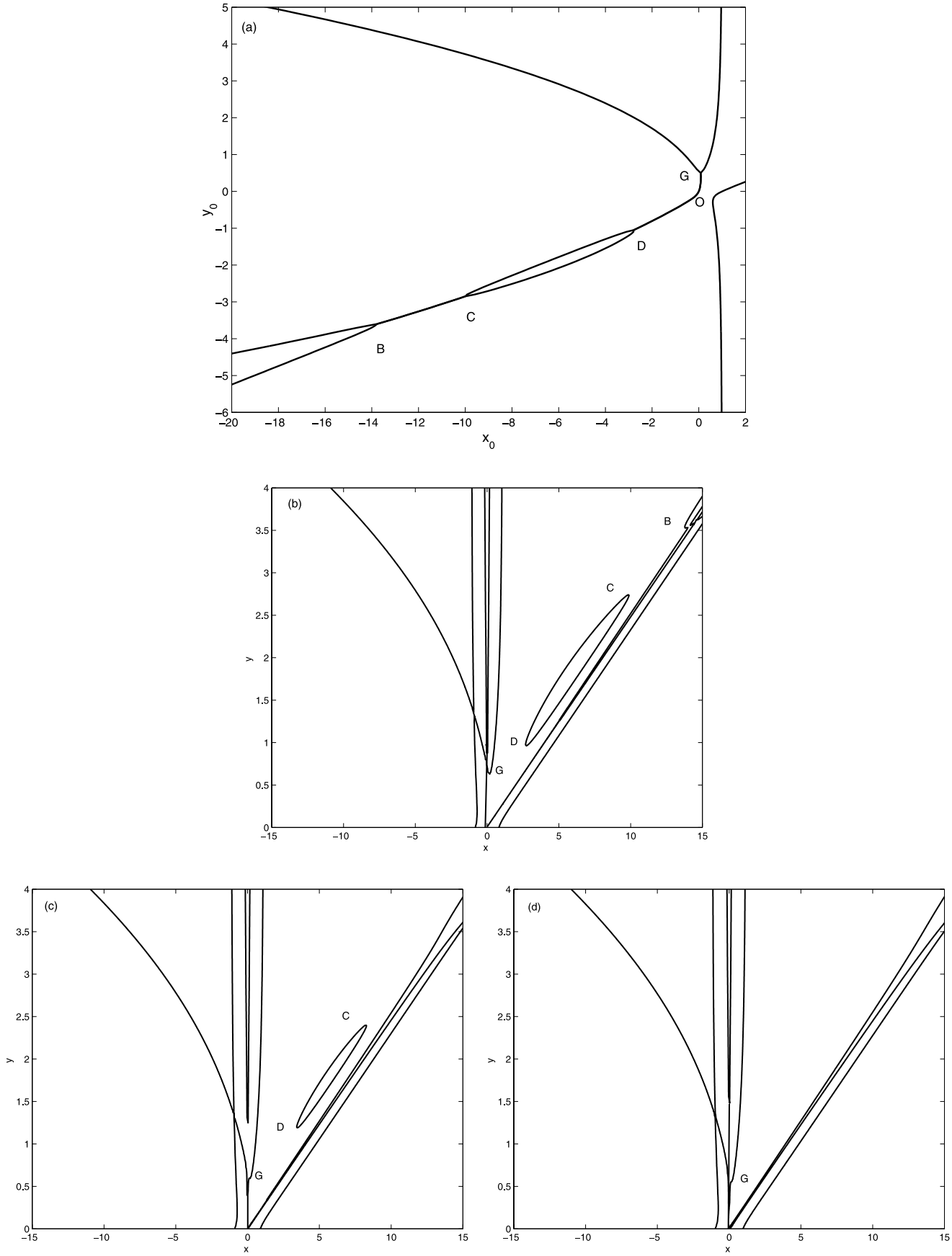

Figure 5. (a) Linear dispersion relation x_0 versus y_0 for a right-hand polarized pump wave with $\eta = 0.2$ and $U = 4$. (b) Nonlinear dispersion relation x versus y for a right-hand polarized pump wave of linearly unstable frequency $x_0 = 0.1025$, with $\eta = 0.2$, $\beta_i = 0.001$, $U = 4$, and $A = 0$, (c) $A = 0.1$, and (d) $A = 0.21$.

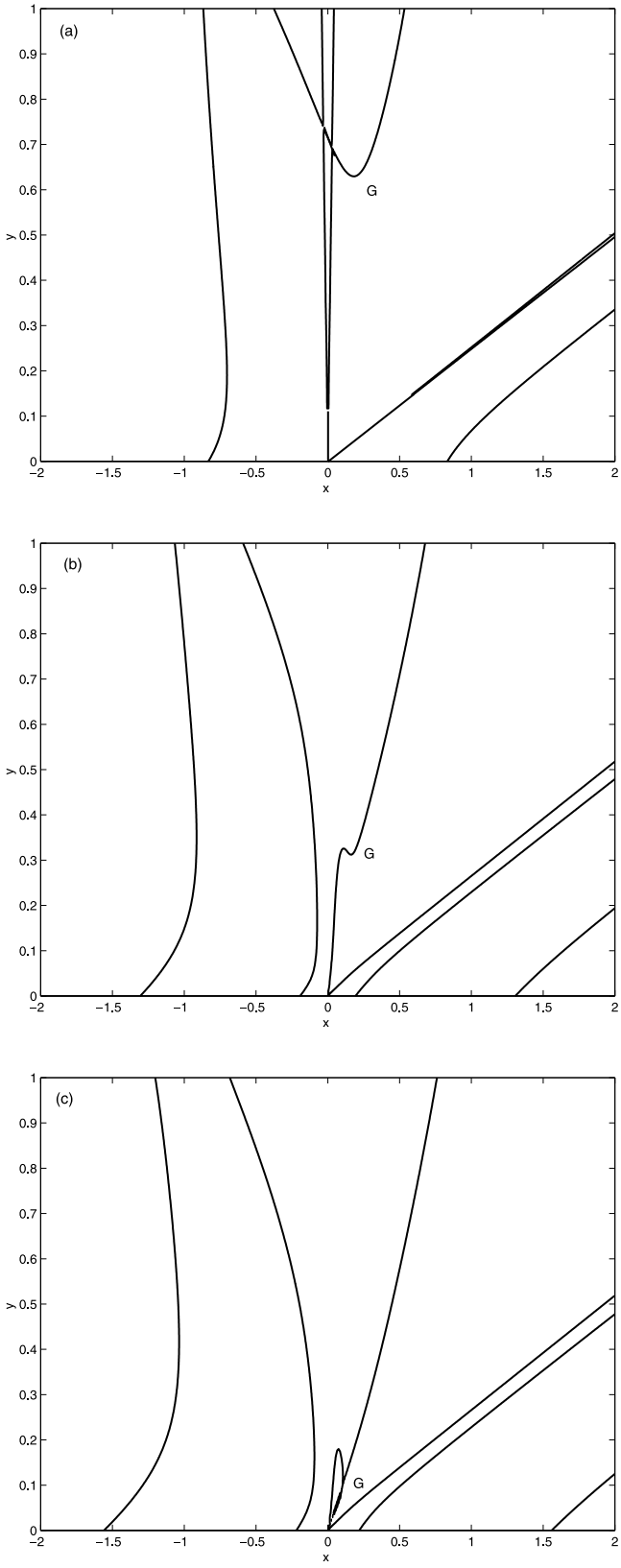

Figure 6. Same as Figure 4b for (a) $A = 0$, (b) $A = 0.8$, and (c) $A = 1.35$.

Table 2. Threshold L-Wave Amplitude, A_t, for Various Pump Wave Frequencies and Temperatures

η	U	x_0	y_0	β_i	A_t	η	U	x_0	y_0	β_i	A_t
0.2	2.2	0.001	0.00131	0.001	0.578	0.2	2.3	0.001	0.001432	0.001	0.805
				0.01	0.573					0.01	0.801
				0.1	0.528					0.1	0.798
				1.0	0.511					1.0	0.780
		0.1	0.1305	0.001	0.586			0.1	0.1366	0.001	0.812
				0.01	0.585					0.01	0.810
				0.1	0.556					0.1	0.810
				1.0	0.554					1.0	0.840
		0.5	0.801	0.001	0.521			0.5	0.811092	0.001	0.693
				0.01	0.497					0.01	0.680
				0.1	0.397					0.1	0.570
				1.0	0.570					1.0	1.420

the large amplitude wave can stabilized the linear instability. This is illustrated in Figure 4. In Table 3, the results are generalized for various temperatures and pump wave frequencies. As it follows from Table 3, A_t increases with decreasing temperature. This behavior is similar to the one encountered in the case of a left-hand polarized large-amplitude wave. In the second case, we assumed that the right-hand pump wave frequency is in a region of linear instability. In this case the large-amplitude wave can destabilize the high-frequency region of the instability, i.e., the region between the pump frequency and D and the region between C and B (see Figure 5). On the other hand, the presence of the pump wave stabilizes the region between the pump wave frequency and O and the region between O and G for $A \geq A_t$ (see Figure 6). In this case, the large-amplitude wave can be triggered by the linear instability itself, and if

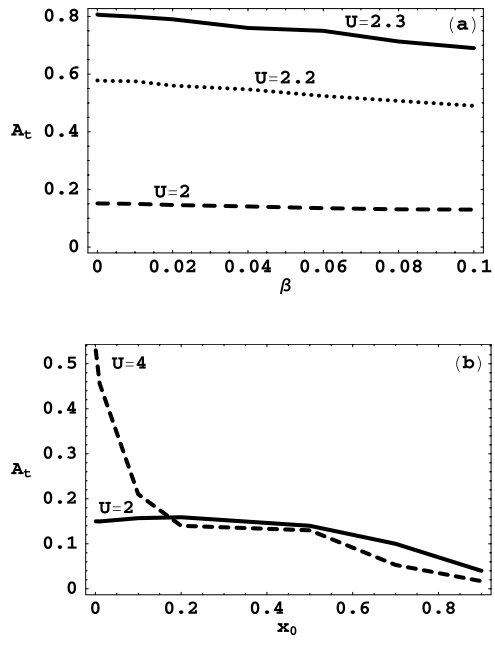

Figure 7. (a) Threshold L-wave amplitude, A_t, versus β_i, for fixed $x_0 = 0.001$ and several U values: $U = 2.0$ (dashed line), $U = 2.2$ (dotted line), and $U = 2.3$ (full line). (b) Threshold L-wave amplitude, A_t, versus frequency, x_0, for fixed $\beta_i = 0.01$, and $U = 2$ (full line), and threshold R-wave amplitude for complete destabilization of the r-instability for the same β_i but $U = 4$ (dashed line).

Table 3. Threshold R-Wave Amplitude, A_t, for Various Pump Wave Frequencies and Temperatures

η	U	x_0	y_0	β_i	A_t
0.2	2.0	0.001	0.00116	0.001	0.153
				0.01	0.151
				0.1	0.135
				1.0	0.100
		0.01	0.011581	0.001	0.151
				0.01	0.150
				0.1	0.134
				1.0	0.110
		0.1	0.112560	0.001	0.144
				0.01	0.142
				0.1	0.123
				1.0	0.100

its amplitude can grow until $A = A_t$, the linear instability can be saturated by the same wave triggered by the instability. In Table 4, these results are extended to various temperatures and pump wave frequencies (for the destabilization mechanism). In this case the threshold A_t value for complete destabilization mechanism follows the same pattern of the stabilization in the preceding cases: A_t decreases with increasing temperature. The stabilization process illustrated in Figure 6 will be discussed in details somewhere else. In general, Tables 2–4 show that the mechanism is valid for a large range of frequencies and temperatures. However, in some cases the A_t values are unrealistically large and, consequently, the mechanism is not efficient [see also *Gomberoff*, 2003]. In Figure 7 we illustrate graphycally some of the content of Tables 2–4.

[20] Thus we have shown that a large amplitude L or R waves can act as a saturation mechanism for r/l-instabilities and, in some cases, it can also lead to a further destabilizing of the linear instabilities, like in the case of a large-amplitude wave with frequency in a linearly unstable region. The unstable region above the large-amplitude wave frequency becomes even more unstable for $A > 0$. Another way of looking at these results is the following. Linear beam-plasma electromagnetic instabilities behave in a different way in the presence of a large-amplitude left-hand or right-hand polarized wave. For example, in the linear theory and in the absence of a large-amplitude wave, in order to trigger the r-instability, the drift velocity of a proton beam

Table 4. Amplitude A_t of the R-Wave, Beyond Which Complete Destabilization of the R-Branch of Beam Instability is Found, for Various Pump Wave Frequencies and Temperatures

η	U	x_0	y_0	β_i	A_t
0.2	4.0	0.01	0.015	0.001	0.461
				0.01	0.456
				0.1	0.412
				0.3	0.318
				1.0	0.091
		0.1	0.0985	0.001	0.212
				0.01	0.210
				0.1	0.184
				0.3	0.134
				1.0	0.025
		2.0	0.806	0.001	0.022
				0.01	0.021
				0.1	0.018
				1.0	0.0021

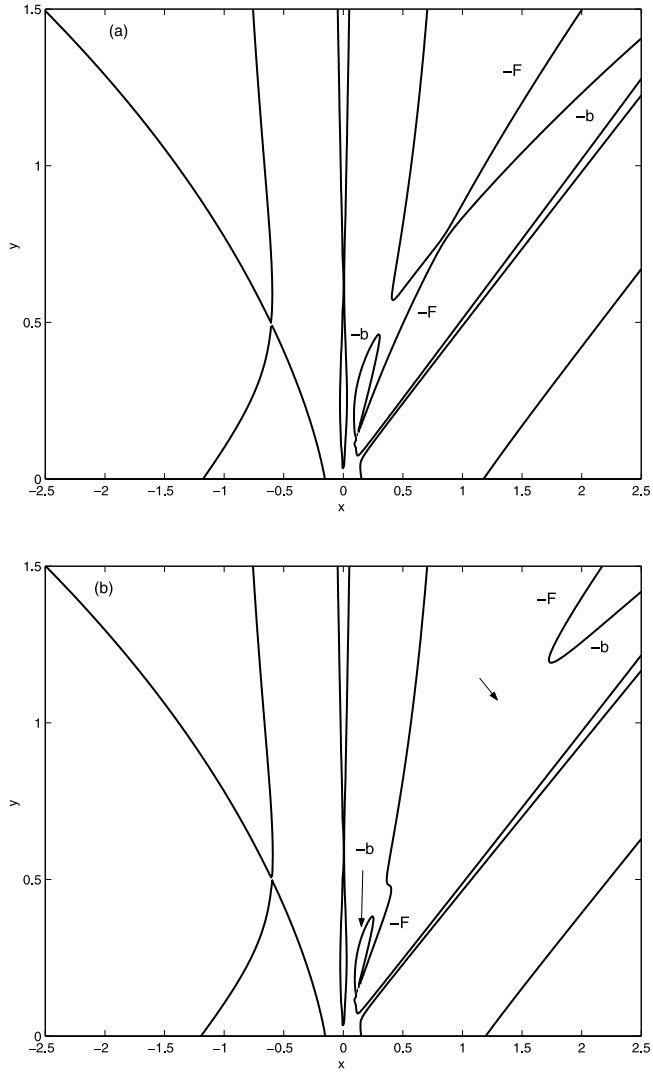

Figure 8. Same as Figure 1, but for (a) $U = 2.0$ and $A_t = 0.16$, showing the stabilization of the linear right-hand instability, and (b) $U = 2.1$ and $A_t = 0.16$, showing the destabilization of the linear instability.

with $\eta = 0.2$ moving in the direction of an external magnetic field must have a drift velocity $U \geq 1.95$ [*Gomberoff and Astudillo*, 1998; *Gomberoff et al.*, 2000]. However, the presence of a large-amplitude polarized wave can stabilize the linear instability when the amplitude satisfies $A \geq A_t$. For the particular case when $U = 2.0$ with the other parameters like in Figure 1, the system is completely stabilized in the presence of an L-wave with $A_t \simeq 0.16$ [*Gomberoff*, 2003]. This result is shown in Figure 8a. This means that in the presence of the L-wave with $A = 0.16$, a larger beam drift velocity is required to trigger the r-instability. In fact, in Figure 8b we have increased from $U = 2.0$ to $U = 2.1$ in order to show that the instability has reappeared, and it is shown by the arrow. Of course if $A \gg A_t$, a much larger drift velocity is required to trigger the instability.

[21] **Acknowledgments.** This work has been partially supported by FONDECYT grants 1020152 and 7020152. One of us (J. H.) thanks MECESUP for a doctoral fellowship.

[22] Shadia Rifai Habbal thanks Bernard J. Vasquez and Manfred P. Leubner for their assistance in evaluating this paper.

References

Cranmer, S. R., Coronal holes and the high speed solar wind, *Space Sci. Rev.*, *101*, 229, 2002.

Daughton, W., S. P. Gary, and Dan Winske, Electromagnetic proton/proton instabilities in the solar wind: Simulations, *J. Geophys. Res.*, *104*, 4657, 1999.

Galvão, R. M. O., G. Gnavi, L. Gomberoff, and F. T. Gratton, Parametric decay of shear Alfvén waves in multicomponent plasmas, *Phys. Rev. E.*, *54*, 4112, 1996.

Gary, S., Electromagnetic ion/ion instabilities and their consequences in space plasmas: A review, *Space Sci. Rev.*, *56*, 373, 1991.

Gnavi, G., L. Gomberoff, F. T. Gratton, and R. M. O. Galvão, Electromagnetic ion-beam instabilities in a cold plasma, *J. Plasma Phys.*, *55*, 77, 1996.

Gomberoff, K., L. Gomberoff, and H. F. Astudillo, Ion-beam plasma electromagnetic instabilities, *J. Plasma Phys.*, *64*, 75, 2000.

Gomberoff, L., Electrostatic waves in the Earth's magnetotail and in comets, and electromagnetic instabilities in the magnetosphere and the solar wind, *IEEE Trans. Plasma Sci.*, *20*, 843, 1992.

Gomberoff, L., Circularly polarized Alfvén and ion cyclotron waves in space plasmas, *Phys. Scr.*, *T60*, 144, 1995.

Gomberoff, L., Ion acoustic damping ffects on parametric decays of Alfvén waves, *J. Geophys. Res.*, *105*, 10,509, 2000.

Gomberoff, L., Stabilization of linear ion beam right-hand polarized instabilities by nonlinear Alfvén/ion-cyclotron waves, *J. Geophys. Res.*, *108*(A6), 1126, doi:10.1029/2003JA009837, 2003.

Gomberoff, L., and H. F. Astudillo, Electromagnetic ion-beam plasma instabilities, *Planet. Space Sci.*, *46*, 1683, 1998.

Gomberoff, L., and R. Elgueta, Resonant acceleration of alpha particles by ion cyclotron waves in the solar wind, *J. Geophys. Res.*, *96*, 9801, 1991.

Gomberoff, L., and R. Hernández, On the acceleration of alpha particles in the solar wind, *J. Geophys. Res.*, *37*, 12,113, 1992.

Gomberoff, L., and R. Neira, Convective growth rates of ion cyclotron waves in a $H^+ - He^+$, and $H^+ - He^+ - O^+$ plasma, *J. Geophys. Res.*, *88*, 2170, 1983.

Gomberoff, L., F. T. Gratton, and G. Gnavi, Excitation and parametric decay of electromagnetic ion cyclotron waves in high speed solar wind streams, *J. Geophys. Res.*, *99*, 14,717, 1994.

Gomberoff, L., F. T. Gratton, and G. Gnavi, Nonlinear decay of electromagnetic ion cyclotron waves in the magnetosphere, *J. Geophys. Res.*, *100*, 1871, 1995.

Gomberoff, L., G. Gnavi, and F. T. Gratton, Minor heavy ions beam-plasma interactions in the solar wind, *J. Geophys. Res.*, *101*, 13,571, 1996.

Gomberoff, L., K. Gomberoff, and A. L. Brinca, Ion acoustic damping effects on parametric decays of Alfvén waves: Right-hand polarization, *J. Geophys. Res.*, *106*, 18,713, 2001.

Gomberoff, L., K. Gomberoff, and A. L. Brinca, New parametric decays of proton beam-plasma electromagnetic waves, *J. Geophys. Res.*, *107*(A7), 1123, doi:10.1029/2001JA000265, 2002.

Hollweg, J. V., Beat, modulational, decay instabilities of a circularly polarized Alfvén wave, *J. Geophys. Res.*, *99*, 23,431, 1994.

Hollweg, J. V., and P. A. Isenberg, Generation of the fast solar wind: A review with emphasis on the resonant cyclotron interaction, *J. Geophys. Res.*, *107*(A7), 1147, doi:10.1029/2001JA000270, 2002.

Hollweg, J. V., R. Esser, and V. Jayanti, Modulational and decay instabilities of Alfvén waves: Effect of streaming He^{++}, *J. Geophys. Res.*, *98*, 3491, 1993.

Hoppe, M. M., C. T. Russell, L. A. Frank, T. E. Eastman, and E. W. Greenstadt, Upstream hydromagnetic waves and their association with backstreaming ion population, *J. Geophys. Res.*, *86*, 4471, 1981.

Hoppe, M. M., C. T Russell, T. E. Eastmann, and L. A. Frank, Characteristics of ULF waves associated with upstream ion beams, *J. Geophys. Res.*, *87*, 643, 1982.

Inhester, B. A., A drift-kinetic treatment of the parametric decay of large amplitude Alfvén waves, *J. Geophys. Res.*, *95*, 10,525, 1990.

Jayanti, V., and J. V. Hollweg, Parametric instabilities of parallel propagating Alfvén waves: Some analytical results, *J. Geophys. Res.*, *98*, 13,247, 1994a.

Jayanti, V., and J. V. Hollweg, On the dispersion relation for parametric instabilities of parallel propagating Alfvén waves, *J. Geophys. Res.*, *98*, 19,049, 1994b.

Leubner, M. D., and A. Viñas, Stability analysis of double picked proton distribution functions in the solar wind, *J. Geophys. Res.*, *91*, 13,366, 1986.

Longtin, M., and B. U. O. Sonnerup, Modulational instability of circularly polarized Alfvén waves, *J. Geophys. Res.*, *91*, 6816, 1986.

Vasquez, V. J., Simulation study of the role of ion-kinetic effects in low frequency wave train evolution, *J. Geophys. Res.*, *100*, 1779, 1995.

L. Gomberoff, Depto. de Física, Facultad de Ciencias, Universidad de Chile, Casilla 653, Santiago, Chile. (lgombero@uchile.cl)

J. Hoyos, Depto. de Física, Facultad de Ciencias, Universidad de Chile, Casilla 653, Santiago, Chile. (jhoyos@fisica.ciencias.uchile.cl)

A. L. Brinca, Centro de Física de Plasmas, Instituto Superior Técnico, 1049-001 Lisboa, Portugal. (ebrinca@alfa.ist.utl.pt)